

Although STL is already available within the R software, `stl()`[7], there are significant drawbacks for researchers using this approach; e.g., they often use the default smoothing parameters, instead of specifying them. To overcome these drawbacks, the authors have developed an algorithm, `stl.fit()`, that selects the best STL model by varying the seasonal and trend smoothing parameters [8]. The choice of the best model is performed by minimizing an error measure. In this case study, the error measure chosen was the Root Mean Square Error (RMSE), although others measures can be chosen, such as the Mean Absolute Percentage Error.

The best data fitting will lead to a model that best describes the stochastic behaviour of the time series; i.e. the one that best captures its dynamics, and so leads to a better inference analysis. The `stl.fit()` procedure will be made available in the R software, so that it is accessible to a wider community, including other fields of research.

The daily satellite products, extracted from MERIS Level 2 reduced resolution images, were aggregated into monthly means, and the missing observations were estimated by linear interpolation.

Overall, the study characterizes the seasonal and trend patterns of the satellite-derived data, and then relates these patterns to environmental changes and possible causes. These components are useful for a better understanding of the temporal variability of the MERIS constituent products at Sagres.

2. DATA AND METHODS

The extraction of the MERIS time series products are described in [4]. The `stl.fit()` was applied to 10 years of monthly MERIS time series for API 1, TSM and YS from Sagres between July 2002 and March 2012 at three sampling Stations A, B and C (Fig.1). The `stl.fit()` procedure was developed and implemented to run under the R software [7] (Fig. 2). After the decomposition of the MERIS time series products, the interquartile range (IQR) was used to assess which component was contributing the most to the observed changes over the time series. An analysis was made of the inter-annual variability in the seasonal component of the MERIS water constituents.

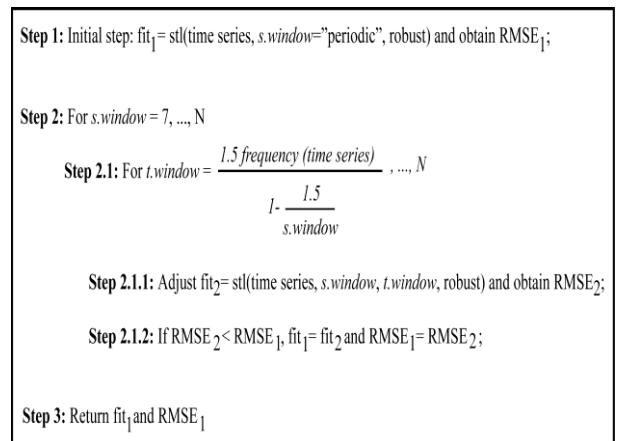


Figure 2. Schematic view of `stl.fit()`, [8].

3. RESULTS

3.1 Decomposing MERIS time series products using `stl.fit()`

For all three Stations, the amplitude of the seasonal term of the API 1, TSM and YS (Fig. 3) decreases, and then increases, towards the end of the of the time horizon. This is most evident for the MERIS API 1 product. The trend component for the three water products shows a marked decrease between July 2002 and March 2004 at Station A.

In terms of IQR (Tab. 1), the seasonal component dominates the observed changes over the time series for the MERIS water constituents (Fig. 3).

Table 1. Dominant components (in bold) based on the interquartile range (%) for the MERIS products at Stations A, B and C.

	Station A			Station B			Station C		
	S _t	T _t	I _t	S _t	T _t	I _t	S _t	T _t	I _t
API	75.1	33.9	76.1	75.3	27.0	19.6	93.6	12.7	27.1
TSM	69.2	27.5	41.5	94.9	26.0	37.4	62.4	24.8	52.2
YS	75.7	32.9	51.2	64.9	28.2	36.6	46.2	18.0	53.4

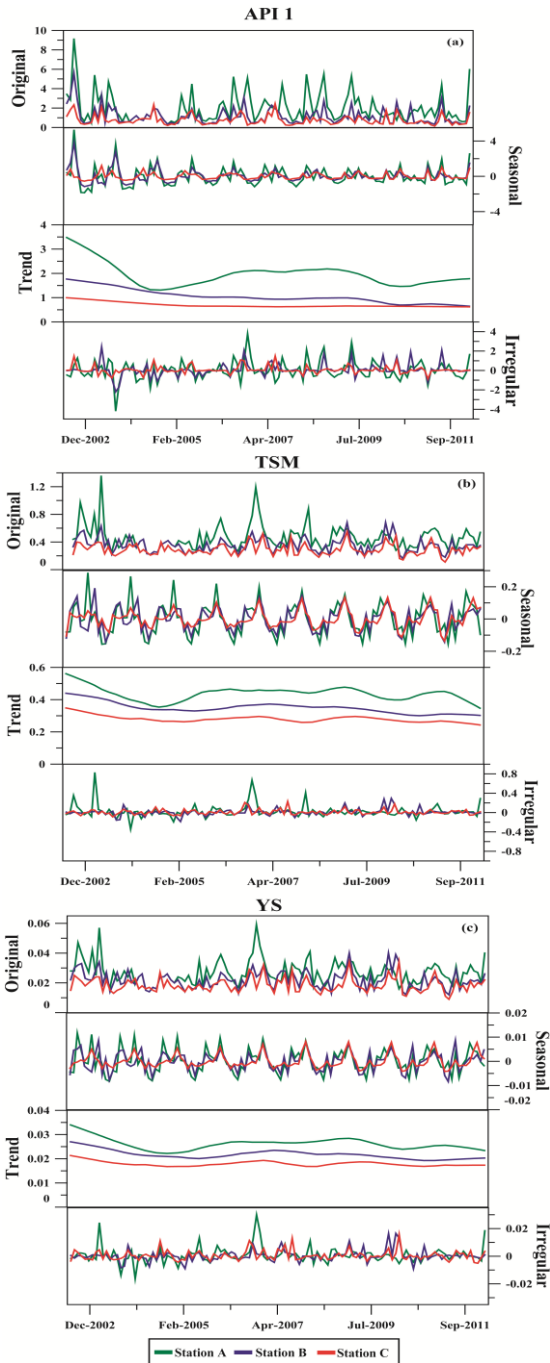


Figure 3. Decomposition plots of MERIS API 1(a), TSM (b) and YS (c) at the three stations using the *stl.fit()*.

3.2 Analysis of the inter-annual variability

The seasonal plot has been used to observe the inter-annual variation of the seasonal component (R function *seasonal()* in the forecast package [9]). The year-to-year variation of the seasonal component can be seen more clearly over time, and thus any marked changes in the seasonal pattern can be easily identified [10].

The seasonal plots show the months with the highest variability at each station decreasing from Station A to Station C for the three water constituents (Fig. 4).

The seasonal variability can be summarised as follows:
 -API 1 at Stations A and B shows high variability in the months of June, December and then between the spring months of March and April, but less pronounced in Station B;
 -TSM and YS at Station A exhibits similar high variability between July to October for TSM and between June to October for YS;
 -TSM and YS products at Station B present notable variations between the months, except for January and November;
 -Station C shows only small changes over the years for the three products (Fig.4).

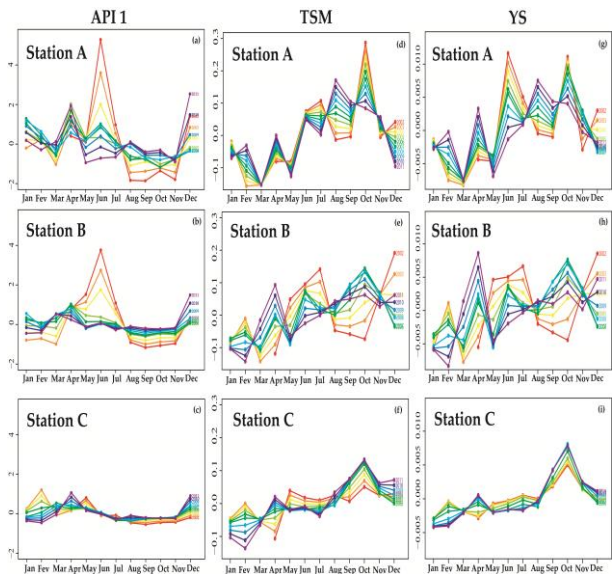


Figure 4. Seasonal variability of the API 1, TSM and YS at Stations A, B and C.

4. DISCUSSION AND CONCLUSIONS

Stl.fit() is a good option for modelling remote sensing time series, particularly, those addressing inter-annual variations.

The decomposition of MERIS water products with *stl.ft()* shows a seasonal component, with increasing dominance from inshore to offshore.

The inter-annual variability for the seasonal component of the MERIS API 1, TSM and YS at the Sagres stations shows the months with the highest variability at each station (see section 3.2). These results provide important information about periods when management action might be needed, for example, for aquaculture activities, or when *in situ* sampling should be made.

Future studies should also take into account the physical and climatic variables that are related to and influenced by the water constituents off Sagres.

5. REFERENCES

1. Zibordi, G., Berthon, J.-F., Mélin, F. & D'Alimonte, D. (2011). Cross-site consistent in situ measurements for satellite ocean color applications: the BiOMaP radiometric dataset. *Remote Sens. Environ.* 115(8), 2104–2115. doi:10.1016/j.rse.2011.04.013
2. Mélin, F., Vantrepotte, V., Clerici, M., D'Alimonte, D., Zibordi, G., Berthon, J.F. & Canuti, E. (2011). Multi-sensor satellite time series of optical properties and chlorophyll-a concentration in the Adriatic Sea. *Prog. Oceanogr.* 91(3), 229–244. doi:10.1016/j.pcean.2010.12.001.
3. Cristina, S. (2016). *Optical Properties of the Ocean and Coastal Waters off the Southwest Coast of Portugal using Satellite Ocean Colour Remote Sensing Data*. U.of Cadiz PhD Thesis. 316pp.
4. Cristina, S., Moore, G.F., Goela, P.R.F.C., Icely, J.D. & Newton, A. (2014). In situ validation of MERIS marine reflectance off the southwest Iberian Peninsula: assessment of vicarious adjustment and corrections for near-land adjacency. *Int. J. Remote Sens.* 35(6), 2347–2377. doi: 10.1080/01431161.2014.894657.
5. Cristina, S., Icely, J., Goela, P.C., DelValls, T.A. & Newton, A. (2015). Using remote sensing as a support to the implementation of the European Marine Strategy Framework Directive in SW Portugal. *Cont. Shelf Res.* 108, 169–177. doi:10.1016/j.csr.2015.03.011.
6. Cleveland, R.B., Cleveland, W.S., McRae, J.E. & Terpenning, I. (1990). Stl: A seasonal-trend decomposition procedure based on loess. *J. Off. Stat.* 6(1), 3–73.
7. R Core Team. (2016). *A language and environment for statistical computing*. R Foundation for Statistical Computing. Vienna, Austria.
8. Cristina, S., Cordeiro, C., Lavender, S., Goela, P.G., Icely, J., Newton, A. (2016). Seasonal-Trend decomposition time series based on Loess applied to MERIS products from the SW Iberian Peninsula: Sagres. *Remote Sens.* Accepted for publication.

9. Hyndman, R. J. (2015). *Forecast: Forecasting functions for time series and linear models*. R package version 6.2.

10. Hyndman R., Athanasopoulos. G. Forecasting: principles and practice. Available Online: <http://otexts.org/fpp/> (accessed on 08 September 2015).

6. ACKNOWLEDGEMENTS

Sónia Cristina and Priscila Costa Goela have been funded by PhD grants from the Portuguese FCT (SFRH/BD/78354/2011 and SFRH/BD/78356/2011, respectively); Alice Newton is funded by EU FP7 project DEVOTES (grant no. 308392); John Icely is funded by EU FP7 AQUA-USER (grant no. 607325), and Horizon 2020 AquaSpace (grant no 633476). Clara Cordeiro is funded by FCT-Fundação para a Ciência e Tecnologia, Portugal, through the project UID/MAT/00006/2013. We also thank ESA and ACRI-ST for access to ODESA MEGS® (<http://earth.eo.esa.int/odesa>).